

# 1 Measurements of global and local polarization of 2 hyperons in 200 GeV isobar collisions from STAR

---

3 **Xingrui Gou, for the STAR Collaboration**

4 *<sup>a</sup>Institute of Frontier and Interdisciplinary Science & Key Laboratory of Particle Physics and Particle  
5 Irradiation (Ministry of Education), Shandong University, Qingdao, Shandong, China*

6 *E-mail: [Gouxr@sdu.edu.cn](mailto:Gouxr@sdu.edu.cn)*

7 In these proceedings, we present the measurements of global polarization for  $\Lambda$ ,  $\bar{\Lambda}$  with the high-  
statistics data collected by the STAR experiment for isobar (Ru+Ru, Zr+Zr) collisions at  $\sqrt{s_{NN}} =$   
200 GeV. These measurements allow us to study possible magnetic field driven effects through  
the polarization difference and system size dependence of global polarization. Furthermore, we  
present the first measurements of  $\Lambda$ ,  $\bar{\Lambda}$  hyperon local polarization in isobar collisions at  $\sqrt{s_{NN}} =$   
200 GeV. Comparisons with previous measurements in Au+Au and Pb+Pb collisions at RHIC  
and LHC provide important insights into the collision system size and energy dependence of the  
vorticities.

*25th International Spin Physics Symposium (SPIN 2023)  
24-29 September 2023  
Durham, NC, USA*

## 1. Introduction

In non-central heavy-ion collisions, the produced system has large orbital angular momentum and may have a strong vortical structure, which leads to the global spin polarization of hyperons through the spin-orbital interaction [1]. Due to the nature of the weak decay,  $\Lambda$  hyperon's polarization can be determined through the angular distribution of decay daughter protons in parent's rest frame. Global polarization has been observed for  $\Lambda$  and  $\bar{\Lambda}$  hyperons in Au+Au collisions from  $\sqrt{s_{NN}} = 3$  to 200 GeV by the STAR experiment [2].

In these proceedings, we report  $\Lambda(\bar{\Lambda})$  global and local polarization as a function of centrality in Ru+Ru and Zr+Zr collisions at  $\sqrt{s_{NN}} = 200$  GeV, using the data collected by STAR experiment.

## 2. Global polarization results

In the STAR experiment, the global polarization is determined by

$$P_{\Lambda} = \frac{8}{\alpha\pi} \frac{1}{A^0} \frac{\langle \sin(\Psi_1 - \phi_p^*) \rangle}{\text{Res}(\Psi_1)}, \quad (1)$$

where  $\alpha$  is the decay parameter,  $A^0$  is the acceptance correction factor,  $\phi_p^*$  is the azimuthal angle of decay proton in  $\Lambda$ 's rest frame. The first order event plane (EP) direction  $\Psi_1$  and the EP resolution  $\text{Res}(\Psi_1)$  are determined using the Zero Degree Calorimeters with Shower Maximum Detectors (ZDC SMD).  $\Lambda(\bar{\Lambda})$  hyperons have been reconstructed through the decay channel:  $\Lambda \rightarrow \pi^- + p$  ( $\bar{\Lambda} \rightarrow \pi^+ + \bar{p}$ ).

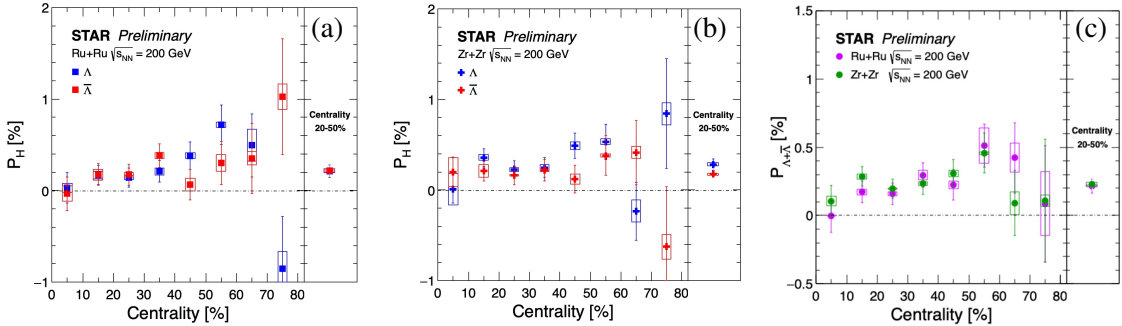


**Figure 1:** Global polarization of  $\Lambda$  and  $\bar{\Lambda}$  as a function of centrality in Ru+Ru(a), Zr+Zr(b) collisions at  $\sqrt{s_{NN}} = 200$  GeV. Panel (c) shows  $\Lambda+\bar{\Lambda}$  global polarization results in isobar collisions. Open boxes and vertical lines represent systematic and statistical uncertainties.

Figure 1 (a) and (b) show  $\Lambda$  and  $\bar{\Lambda}$  global polarization  $P_{\Lambda, \bar{\Lambda}}$  as a function of centrality in Ru+Ru and Zr+Zr collisions. The polarization increases from central to peripheral collisions. In order to achieve a better precision in polarization splitting, we also combine measurements in 20-50% centrality. No significant difference between  $\Lambda$  and  $\bar{\Lambda}$  global polarization in Ru+Ru and Zr+Zr collisions is observed. It indicates that there is no magnetic field driven effect on the hyperon polarization within present statistical precision. Figure 1 (c) shows  $\Lambda+\bar{\Lambda}$  global polarization  $P_{\Lambda+\bar{\Lambda}}$  as a function of centrality in Ru+Ru and Zr+Zr collisions. The results are consistent in each centrality between Ru+Ru and Zr+Zr collisions.

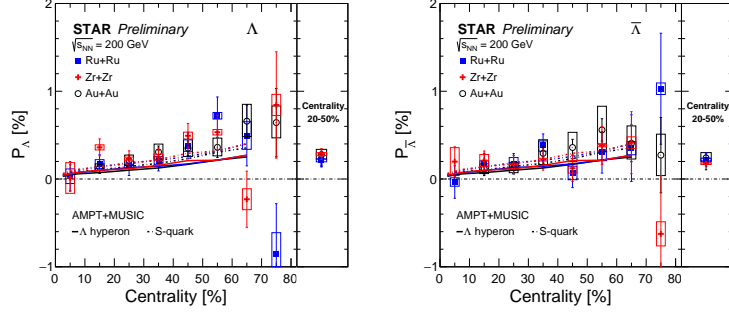


**Figure 2:**  $\Lambda$ (left) and  $\bar{\Lambda}$ (right) global polarization as a function of centrality in Ru+Ru, Zr+Zr, and Au+Au collisions at  $\sqrt{s_{NN}} = 200$  GeV.

Figure 2 shows  $\Lambda$  and  $\bar{\Lambda}$  global polarization comparison between isobar and Au+Au collisions. The results are consistent for the whole centrality range, indicating there is no obvious collision system size dependence. The hydrodynamic model calculations from  $\Lambda$  polarization scenario and  $s$ -quark polarization scenario are consistent with the experiment data[3].

### 3. Local polarization results

The component of the polarization along the beam direction can be measured by

$$\langle \cos\theta_p^* \rangle = \int \frac{dN}{d\Omega^*} \cos\theta_p^* d\Omega^*, \quad (2)$$

where  $\theta_p^*$  is the polar angle of the daughter proton in the  $\Lambda$  rest frame [4].

STAR has measured the local polarization with respect to the second-order event plane in Au+Au collisions at  $\sqrt{s_{NN}} = 200$  GeV. The local polarization  $\langle \cos\theta_p^* \rangle$  as a function of azimuthal angle relative to the second-order event plane shows a sine modulation, as expected from quadrupole structure of vorticity along the beam direction.

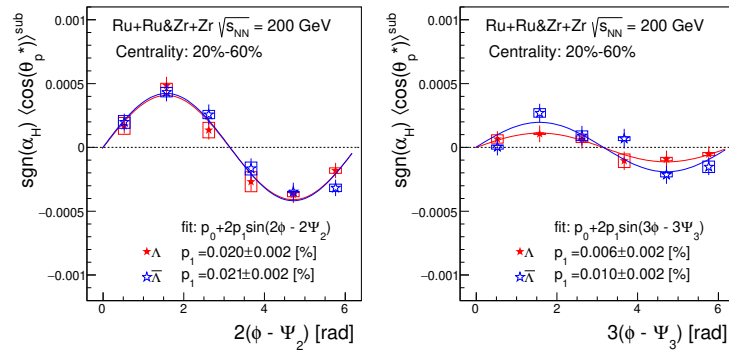


**Figure 3:** Local polarization  $\langle \cos\theta_p^* \rangle$  of  $\Lambda$  and  $\bar{\Lambda}$  hyperons as a function of azimuthal angle  $\phi$  relative to the second and third-order event plane in isobar collisions at  $\sqrt{s_{NN}} = 200$  GeV.

Figure 3 shows  $\langle \cos\theta_p^* \rangle$  of  $\Lambda$  and  $\bar{\Lambda}$  hyperons as a function of azimuthal angle  $\phi$  relative to the second-order event plane  $\Psi_2$ (left) and third-order event plane  $\Psi_3$ (right) for 20% – 60% centrality,

45 respectively, in isobar collisions at  $\sqrt{s_{NN}} = 200$  GeV. The second and third-order event planes are  
 46 determined by the Time Projection Chamber detector (TPC). The solid lines are the fits to the results  
 47 with  $p_0 + 2p_1 \sin(n\phi - n\Psi_n)$ . The left panel in figure 3 shows a clear sine modulation in polarization  
 48 signal, as expected from quadrupole structure of vorticity along the beam direction. The pattern in  
 49 isobar collisions is similar to that in Au+Au with better statistical significance. Figure 3 (right)  
 50 shows the first measurements of  $\langle \cos\theta_p^* \rangle$  with respect to the third-order event plane  $\Psi_3$ . The results  
 51 also show a sine modulation for both  $\Lambda$  and  $\bar{\Lambda}$ , indicating triangular flow driven polarization[5].

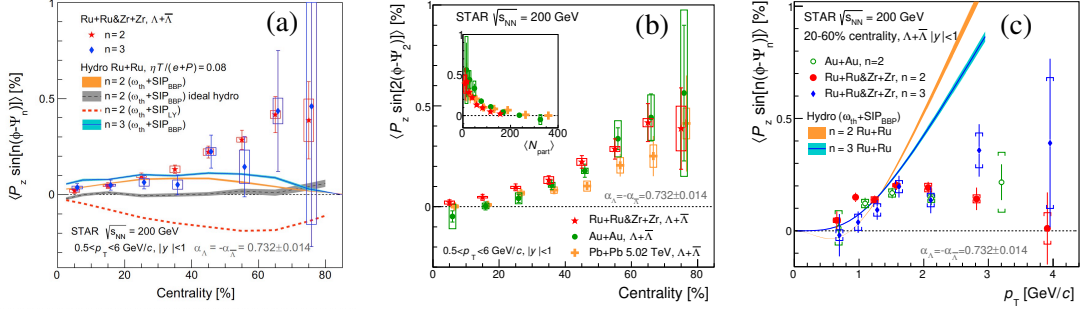


**Figure 4:** (a): the local polarization w.r.t 2nd(3rd) event plane of  $\Lambda + \bar{\Lambda}$  as a function of the collision centrality in isobar collisions at  $\sqrt{s_{NN}} = 200$  GeV. (b): the comparison of the second Fourier sine coefficient of  $\Lambda + \bar{\Lambda}$  local polarization among isobar, Au+Au collisions at  $\sqrt{s_{NN}} = 200$  GeV and Pb+Pb collisions at  $\sqrt{s_{NN}} = 5.02$  TeV. (c): local polarization w.r.t 2nd(3rd) event plane of  $\Lambda + \bar{\Lambda}$  as a function of transverse momentum.

52 Figure 4 (a) presents the comparison of centrality dependence of magnitude of  $\Lambda + \bar{\Lambda}$  local polar-  
 53 ization with respect to second and third EPs. The results from second order event plane increase  
 54 in magnitude towards peripheral collisions, similar to the behavior of elliptic flow. The results  
 55 from third order also increase from central to peripheral collisions. However, there is no signif-  
 56 icant difference between the second-order and third-order local polarization within measurement  
 57 uncertainties.

58 Figure 4 (b) shows the  $\Lambda + \bar{\Lambda}$  local polarization with respect to the second-order event plane as  
 59 a function of the collision centrality in isobar, Au+Au, and Pb+Pb collisions[6]. A hint of system  
 60 size dependence has been observed when compared isobar, Au+Au collisions at  $\sqrt{s_{NN}} = 200$  GeV,  
 61 while the collision energy dependence is not obvious between  $\sqrt{s_{NN}} = 200$  GeV Au+Au collisions  
 62 and  $\sqrt{s_{NN}} = 5.02$  TeV Pb+Pb collisions.

63 The local polarization relative to both event planes are plotted as a function of hyperons' trans-  
 64 verse momentum in Figure 4 (c). Results show that  $p_T$  dependence of the polarization is indeed  
 65 similar to that of elliptic ( $v_2$ ) and triangular ( $v_3$ ) flow.

#### 66 4. Summary

67 The global and local polarization of  $\Lambda$  and  $\bar{\Lambda}$  have been measured in isobar (Ru+Ru, Zr+Zr)  
 68 collisions at  $\sqrt{s_{NN}} = 200$  GeV. The global polarization of  $\Lambda$  and  $\bar{\Lambda}$  are consistent, indicating that the  
 69 magnetic field effects on global polarization are not observed within current statistical limitation.  
 70 The global polarization is consistent across collisions with different system sizes, Ru+Ru, Zr+Zr,

71 and Au+Au at same beam energy. Significant local polarization signals with respect to the second-  
72 order and third-order event plane are observed in isobar collisions at  $\sqrt{s_{NN}} = 200$  GeV. A slight hint  
73 of collision system size dependence has been observed, while energy dependence is not obvious.

#### 74 **Acknowledgements**

75 The author is supported by the National Key Research and Development Program of China  
76 (Grant No. 2022FYA1604903)

#### 77 **References**

- 78 [1] Z. T. Liang and X. N. Wang, Phys. Rev. Lett. 94,102301 (2005); 96, 039901(E) (2006).  
79 [2] L. Adamczyk et al., (STAR Collaboration), Nature 548, 62 (2017).  
80 [3] B. Fu et al, arXiv: 2201.12970 (2022).  
81 [4] J. Adam et al., (STAR Collaboration), Phys. Rev. Lett. 123, 132301(2019)  
82 [5] J. Adam et al., (STAR Collaboration), Phys. Rev. Lett. 131, 202301(2023)  
83 [6] S. Acharya et al., (ALICE Collaboration), Phys. Rev. Lett. 128 (2022) 17, 172005.  
84 [7] J. Adam et al., (STAR Collaboration), Phys.Rev.C 108 1, 014910 (2023).